

# General Relativity effects and line emission

Giorgio Matt \*

Dipartimento di Fisica, Università Roma Tre, Via della Vasca Navale 84, I-00146 Roma, Italy

Received 30 May 2005, accepted 11 Nov 2005

Published online later

**Key words** accretion, accretion disks – relativity – line: profiles – galaxies: active – X-rays: binaries

General Relativity effects (gravitational redshift, light bending, ...) strongly modify the characteristics of the lines emitted close to the Black Hole in Active Galactic Nuclei and Galactic Black Hole systems. These effects are reviewed and illustrated, with particular emphasis on line emission from the accretion disc. Methods, based on the iron line, to measure the two astrophysically relevant parameters of a Black Hole, the mass and spin, are briefly discussed.

© 2006 WILEY-VCH Verlag GmbH & Co. KGaA, Weinheim

## 1 Introduction

With the advent of X-ray missions carrying on-board high sensitivity, moderate energy resolution instruments (the first of which being ASCA, followed by *BeppoSAX*, *Chandra*, *XMM-Newton* and now *Suzaku*), probing General Relativity (GR) effects on iron emission lines has become a reality, and it is now an important part of the studies on Active Galactic Nuclei (AGN) and Galactic Black Hole systems (GBH).<sup>1</sup>

In this paper I will review the main GR effects, and I will discuss how they can be used to measure the two astrophysically relevant parameters of a Black Hole, the mass and the angular momentum (“spin”). The paper is organized as follows: in Sec. 1 the basic concepts concerning Black Holes, of relevance for understanding GR effects on line emission, are summarized. In Sec. 2 I will discuss line emission from a relativistic accretion disc, while Sec. 3 is devoted to the discussion of the strengths and weaknesses of methods, based on iron emission lines, to measure the mass and spin of the Black Hole. Conclusions are given in Sec. 4.

For a complete treatment of Black Holes the reader is deferred to standard textbooks like e.g. the ones by Misner et al. (1973) and Chandrasekhar (1983), or to classical papers like Bardeen et al. (1972). See also Fabian et al. (2000) and Reynolds & Nowak (2003) for reviews on the iron line properties from relativistic accretion discs.

## 2 Black Holes

A Black Hole (BH) or, better, the space-time around it, is fully characterized by only three quantities: its mass  $M$ , angular momentum  $J$  and electric charge  $Q$ . The latter is usu-

ally assumed to be negligible for astrophysically relevant Black Holes. The space time around a BH is described by the Kerr-Newman metric which, when  $Q=0$ , reduces to the slightly simpler Kerr metric. If also  $J$  is null, than the metric is the much simpler Schwarzschild one. It may be interesting to remember that, while the static solution was found by Karl Schwarzschild in 1916 (i.e., only one year after the publication by Einstein of his theory of General Relativity), the rotating solution was found by Roy Kerr only in the sixties (Kerr 1963), which possibly tells us more on the lack of interest in the field rather than on the mathematical difficulty of the problem (which was of course far from trivial).

All relevant General Relativity effects around a BH are scale invariant, i.e. do not depend on the BH mass. It is therefore convenient to measure all distances in units of the so-called gravitational radius,  $r_g = GM/c^2$ . It is also useful to introduce the adimensional angular momentum per unit mass,  $a = Jc/GM^2$ , called for simplicity “spin” here-in-after.

In Boyer–Lindquist spherical coordinates (namely  $t, r, \phi, \theta$ , with the usual meaning of symbols), the Kerr metric can be written as:

$$ds^2 = - \left( 1 - \frac{2r}{\Sigma} \right) dt^2 - \left( \frac{4ar \sin^2 \theta}{\Sigma} \right) dt d\phi + \left( \frac{\Sigma}{\Delta} \right) dr^2 + \Sigma d\theta^2 + \left( r^2 + a^2 + \frac{2a^2 r \sin^2 \theta}{\Sigma} \right) \sin^2 \theta d\phi^2 \quad (1)$$

where:

$$\Sigma = r^2 + a^2 \cos^2 \theta; \quad \Delta = r^2 - 2r + a^2 \quad (2)$$

(If the Black Hole electric charge is not null, then, in geometrized units,  $\Delta = r^2 - 2r + a^2 + Q^2$ ). For  $a=0$ , the Schwarzschild metric is obtained:

\* e-mail: matt@fis.uniroma3.it

<sup>1</sup> Relativistically distorted iron lines from accretion discs around neutron stars have also possibly been observed, e.g. Di Salvo et al. (2005).

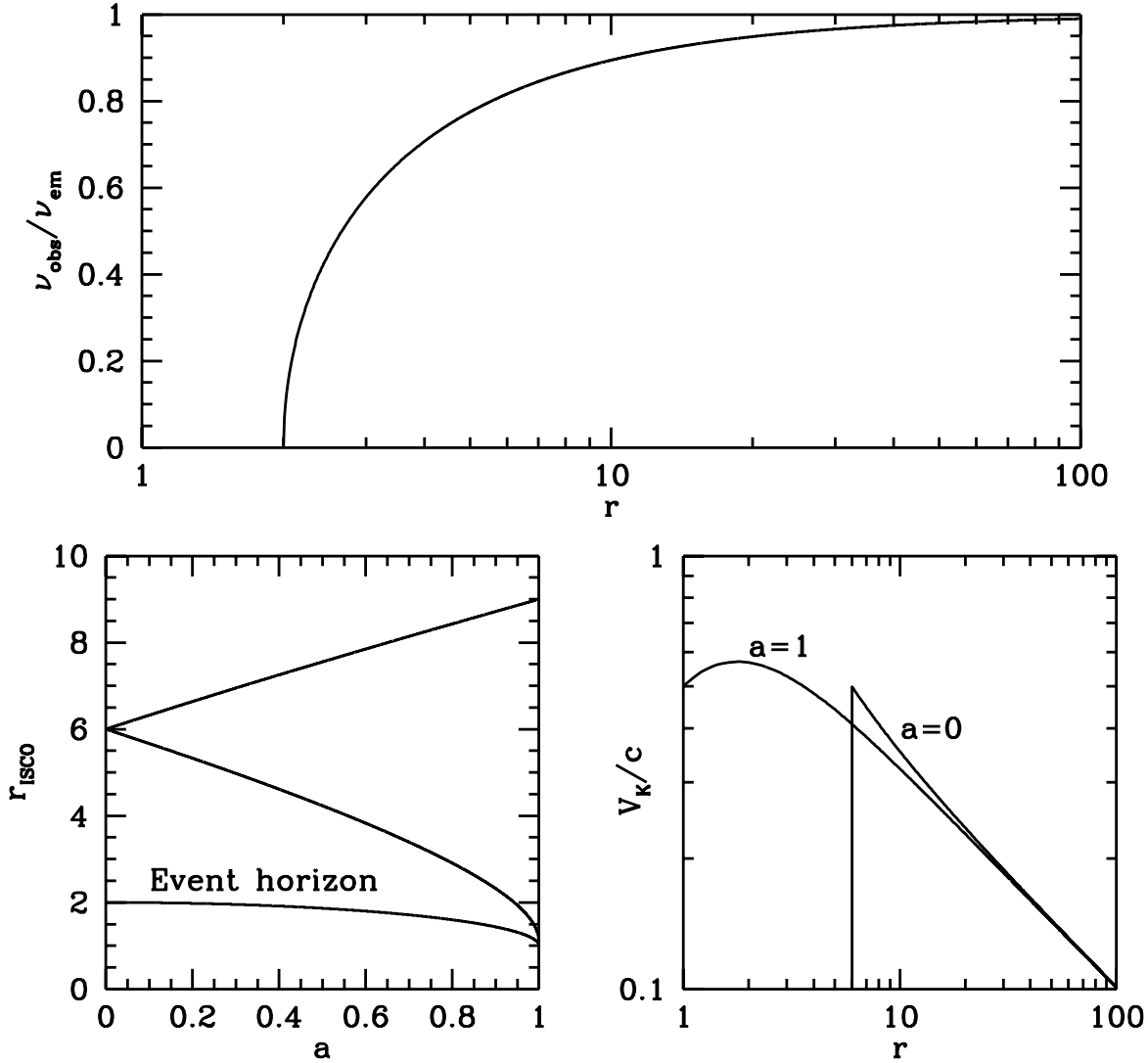


**Fig. 1** Upper panel: the ratio between the observed and emitted frequency of a photon (“gravitational redshift”) in Schwarzschild metric as a function of the radius at which the photon is emitted. Lower-left panel: the radius of the Innermost Stable Circular Orbit as a function of the BH spin. The lower (upper) curve refers to a co- (counter-) rotating disc. The radius of the Event Horizon is also shown for comparison. Lower-right panel: the Keplerian velocity (in the LNRF) in the equatorial plane as a function of radius, for a static and a maximally rotating BH.

$$ds^2 = - \left(1 - \frac{2}{r}\right) dt^2 + \left(1 - \frac{2}{r}\right)^{-1} dr^2 + r^2 (d\theta^2 + \sin^2 \theta d\phi^2) \quad (3)$$

The radius of the Event Horizon, i.e. the surface of “no return”, is given by  $R_{EO} = 1 + \sqrt{1 - a^2}$ . This implies that  $0 \leq a \leq 1$ , i.e. that there is a maximum value for the spin. When  $a=1$  the BH is said to be maximally rotating; in this case the radius of the Event Horizon is equal to the gravitational radius, while it is  $2r_g$  (the “Schwarzschild radius”) for

a static ( $a=0$ ) BH.<sup>2</sup> It is interesting to note that the Schwarzschild radius corresponds, in a pure Newtonian calculation, to the radius a star should have in order than at its surface the escape velocity is equal to  $c$ . Indeed, Black Holes (or invisible stars, as they were called at the time) were predicted in this way more than two centuries ago by Michell (1783) and Laplace (1796), even if of course they could not imag-

<sup>2</sup> It is important to recall here that Thorne (1974) has shown that in the standard accretion disc model the radiation emitted by the disc and swallowed by the BH produces a counteracting torque which limits the spin to a maximum value of  $\sim 0.988$ , corresponding to  $R_{EO} \sim 1.23$ .

ine that from such objects nothing, not only the light, could escape.

An important General Relativity effect is the gravitational redshift. Photons get out of the gravitational potential of the BH only by losing energy, being therefore redshifted. In Schwarzschild metric:

$$\nu_{obs}/\nu_{em} = \sqrt{1 - \frac{2}{r}} \quad (4)$$

where  $\nu_{em}$  and  $\nu_{obs}$  are the emitted and observed (at infinity) frequencies of the photon, and  $r$  the emission radius (see also Fig. 1). In Kerr metric, a similar formula can be written only for the photons emitted on the rotation axis, where it reads:

$$\nu_{obs}/\nu_{em} = \sqrt{1 - \frac{2r}{r^2 + a^2}} \quad (5)$$

For any other point, the “dragging of the inertial frame”, i.e. the corotation of the space-time with the BH spin makes gravitational and Doppler shifts not separable.

### 3 Line emission from accretion discs

#### 3.1 General and historic remarks

Accretion on Black Holes, at least for bright systems, it is widely believed to occur via an accretion disc, where gravitational energy can be efficiently dissipated and eventually converted into radiation. Accretion discs are very complicated systems, and the details of the physical processes are far from being fully understood. For what follows, however, we only have to assume: that the disc is geometrically thin (i.e. its height is always much smaller than its radius at any radius), so that it may be approximated with a thin slab on the equatorial plane; that it is homogenous enough in order that clumpiness does not affect much the line emissivity; and that it is optically thick, so that iron line fluorescent emission can be efficient. (Even these assumptions, however, may be questionable and have indeed been questioned several times. This however is not the place to discuss when and how the results are modified releasing one or more of them).

I also assume that the iron line is due to fluorescent emission following illumination (and photo-ionization) of the accretion disc by an external source of X-rays. George & Fabian (1991) and Matt et al. (1991) discussed in detail the properties of the fluorescent line for neutral matter, while Matt et al. (1993a, 1996), Nayakshin & Kallman (2001) and A.C. Fabian, R.R. Ross and collaborators in a series of papers (Ross & Fabian 2005, and references therein) discussed the case of ionized matter.

GR effects on the radiation emitted by an accretion disc were first studied by Cunningham (1975), while Fabian et al. (1989) and Chen et al. (1989) were the first to model line emission from relativistic discs and compare calculations with observations. Different groups (too many to be quoted here; further references can be found in: Fabian et

al. 2000; Reynolds & Nowak 2003; Fabian & Miniutti 2005; Karas, this volume) have since then performed calculations of line profiles under different assumptions and physical conditions, mainly stimulated by the *GINGA* discovery that iron lines are almost ubiquitous in the X-ray spectra of AGN (e.g. Nandra & Pounds 1994). Models of line profiles from accretion discs are also present in the widely used XSPEC software package (Arnaud 1996)<sup>3</sup> for X-ray spectral fitting. For many years the only models available in XSPEC were the DISKLINE (Fabian et al. 1989) and LAOR (Laor 1991) models. The DISKLINE model is fast and reliable, but it is valid only in Schwarzschild metric and it is somewhat inaccurate, in particular for small radii and large inclination angles, because of the straight line approximation for the photon geodesics. The LAOR model is valid only for a maximally rotating black hole; it is fast and reliable, but it is based on a rather coarse grid of parameters. The limitations to these two codes were obviously due to the limited power of the computers at the time they were written: more detailed fitting codes would simply have been unmanageable. Computers improved a good deal since then, and now fully relativistic codes in Kerr metric (allowing for the entire range of spin) have become publically available even if not yet included in the standard XSPEC release: the KY (Dovciak et al. 2004a,b) and KD (Beckwith & Done 2004, 2005) suits.<sup>4</sup>

#### 3.2 Relativistic discs and line emission

The inner radius of the accretion disc cannot be smaller than the Innermost Stable Circular Orbit (ISCO). This of course does not mean that there is no matter at radii lower than the ISCO; simply, the matter must spiral in (see Krolik & Hawley 2002 for different definitions of the “edge” of the disc). The ISCO depends on the BH spin and on whether the disc is co- or counter-rotating with the BH (see Fig. 1):

$$r_{ISCO} = 3 + Z_2 \pm [(3 - Z_1)(3 + Z_1 + 2Z_2)]^{\frac{1}{2}} \quad (6)$$

where

$$Z_1 = 1 + (1 - a^2)^{\frac{1}{3}}[(1 + a)^{\frac{1}{3}} + (1 - a)^{\frac{1}{3}}]$$

$$Z_2 = (3a^2 + Z_1^2)^{\frac{1}{2}}$$

The  $- (+)$  sign applies to co- (counter-) rotating discs. Indeed, the decrease of the ISCO with  $a$  (for a corotating disc) provides a method to measure the spin (see next section).

Motion of matter in accretion discs is supposed to be dominated by the gravitational potential of the BH, and then rotation to be Keplerian. Close to the BH the Keplerian velocity,  $v_K$ , becomes very large, reaching a significant fraction of the velocity of light. In the Locally Non-Rotating

<sup>3</sup> see also <http://xspec.gsfc.nasa.gov/>

<sup>4</sup> Just before submitting this contribution, Brenneman & Reynolds (2006) presented one new fully relativistic code for spectral fitting in XSPEC.

Frame (LNRF), i.e. the reference frame “rotating with the Black Hole” (Bardeen et al. 1972), we have (see also Fig. 1):

$$v_K/c = \frac{r^2 - 2a\sqrt{r} + a^2}{(r^2 + a^2 - 2r)^{\frac{1}{2}} (r^{3/2} + a)} \quad (7)$$

It is interesting to note that  $v_K$  can be as high as almost half the velocity of light, implying that the Doppler shift and boosting may be very prominent (Doppler boosting is the brightening/dimming of the flux when the matter is approaching/receding. It is a Special Relativity aberration effect due to the fact that  $I_\nu/\nu^3$  is a Lorentz invariant). At these velocities, Special Relativity corrections of the Doppler effect must be included, with the result that transverse Doppler effect (i.e. the redshift of photons when matter has only a transverse component of the velocity) is by no means negligible.

In General Relativity, photon geodesics are no longer straight lines (the so-called “light bending”). In Schwarzschild metric they still lie on a plane, and therefore the equation of the orbit can be written in terms of only two coordinates, the radius and the azimuthal angle,  $\Phi$ , on the plane of the trajectory. The differential equation describing the orbit is (Misner et al. 1973):

$$\frac{d^2u}{d\Phi^2} = 3u^2 - u \quad (8)$$

where  $u = 1/r$ . In Kerr metric the orbits are fully three-dimensional, and the equation of motion much more complex (Carter 1968). As a result of light bending, geodesics of photons emitted in the far side of the disc are strongly curved making the disc appears as “bended” towards the observer, with a sort of sombrero-like shape (see e.g. Luminet 1979, 1992).

All these effects strongly modify the properties of emission lines. Let us for simplicity neglect natural and thermal line broadening, so that the line profile, in the matter reference frame, is a  $\delta$ -function. Given the topic of this conference, let us also assume that the line is the neutral iron  $K\alpha$  at 6.4 keV.<sup>5</sup> In Fig. 2 (left panel) the line emission from an annulus at  $r=6$ , seen with an inclination of  $30^\circ$ , is shown after having divided the annulus in azimuthal intervals, with  $\Delta\phi=30^\circ$ . The uppermost panel on the left side refers to matter moving transversally on the near side of the disc ( $\phi=0^\circ$ ). Even in this case, when classic Doppler effect is null, emission is significantly redshifted due to the combination of gravitational and transverse Doppler effects. Going down on the left side, matter starts receding and classic Doppler effect adds to further shift redwards the energy of the photon, which is maximum for  $\phi=90^\circ$ , where instead the flux is minimum due to Doppler (de-)boosting. In the right panels, matter is instead approaching, but even for  $\phi=270^\circ$ ,

when the maximum line-of-sight velocity is attained, emission is globally redshifted because the Doppler effect (for so small radius and inclination angle) cannot fully compensate for gravitational redshift. Due to Doppler boosting, flux is maximum at  $\phi=270^\circ$ . The azimuthally averaged line profile is shown in Fig. 2 (right-upper panel) while the medium and lower right panels show the  $60^\circ$  and  $85^\circ$  inclination angle cases, respectively. Note that at higher inclinations the “blue” peak of the line profile is actually blueshifted with respect to the rest frame energy, because of the larger Doppler effect. Note also that, in the  $85^\circ$  case, structures in between the red and blue peaks appear, due to the bending of the photons emitted on the far side of the disc (e.g. Matt et al. 1993b). This effect is better illustrated in Fig. 3, when the flux and centroid energy of the line as a function of the azimuthal angle are shown for inclination angles of  $30^\circ$  and  $85^\circ$  ( $r=6$ ). While in the  $30^\circ$  case the variations in flux are dominated by the Doppler boosting, in the  $85^\circ$  case the peak of the emission occurs at  $\phi \sim 180^\circ$  due to the strong light bending.

Line profile is further modified by integration over the entire disc. To do that, a crucial ingredient is the radial emissivity law,  $\xi$ . For the iron fluorescent line, which is emitted following external illumination (e.g. George & Fabian 1991; Matt et al. 1991),  $\xi$  depends mainly on the geometry of the system. It is customary to assume a power law emissivity law,  $\xi \propto r^{-q}$ . If  $q < 2$ , the outer regions dominate the emissivity, while the inner regions prevail for  $q > 2$ . Fig. 4 (left panel) show the impact on line profiles of different choices of  $q$ . The right panel instead show, for a given value of  $q$  ( $=2$ ) the line profiles for different values of the outer radius of the emitting region ( $r_{\text{out}}=10, 50, 400 r_g$ ).

Actually, the emissivity law is likely to be more complex than a simple power law. Even in the simplest case, the so-called “lamp-post” model in which the primary emitting region is a small cloud on the BH axis (as in aborted jet models, e.g. Ghisellini et al. 2004), the emissivity law is, neglecting GR effects and radiative transfer subtleties, given by:  $\xi \propto (h^2 + r^2)^{-\frac{3}{2}}$ , where  $h$  is the height of the emitting point;  $\xi$  is then a power law ( $q=3$ ) only for large radii. Once the effects on the emissivity of the incident angle (Matt et al. 1991) and, especially, of GR (light bending, gravitational shift) are included, the emissivity is significantly modified (e.g. Martocchia & Matt 1996, Martocchia et al 2000, 2002). As noted by Martocchia et al. (2002), the steep emissivity law found for the iron line emission of the Seyfert 1 galaxy MCG–6–30–15, as observed by XMM–Newton (Wilms et al. 2001), can be explained by this “geometrical” effect. A more general case, in which the emitting region is no longer forced to stay on the BH axis, has been studied by Miniutti et al. (2003, and this volume).

## 4 Measuring the spin and mass of BHs

Iron line profiles from relativistic accretion discs provides potentially very powerful methods to measure the mass and

<sup>5</sup> This line is actually a doublet, with energies of 6.4055 and 6.3916 keV and a branching ratio of  $\sim 2:1$  (Palmeri et al. 2003). As the broadening effects we are discussing here are much larger than the  $\sim 14$  eV intrinsic separation, we will assume a single narrow line with a weighted mean energy of 6.4 keV).

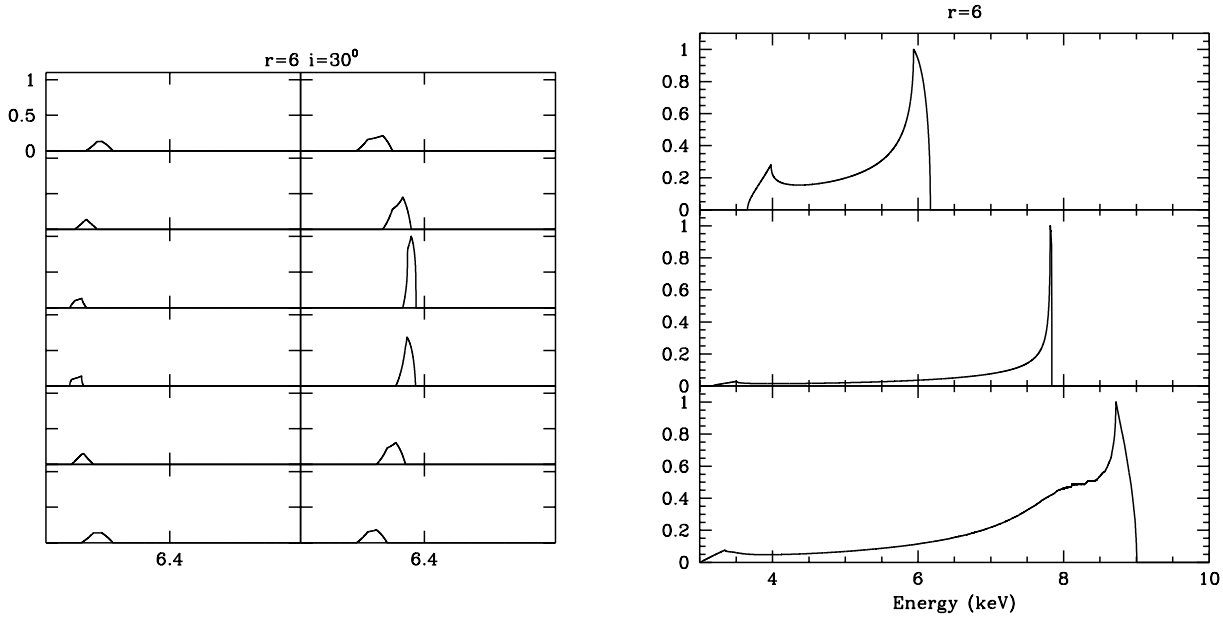


**Fig. 2** *Left panel:* Iron line emission from an annulus at  $r=6$ , seen with an inclination of  $30^\circ$ . Each panel refers to an azimuthal interval with  $\Delta\phi=30^\circ$ . The uppermost panel on the left side refers to matter moving transversally on the near side of the the disc ( $\phi=0^\circ$ ).  $\phi$  increases from top to bottom. Left panels refer to receding matter, right panels to approaching matter. *Right Panel:* Azimuthally-averaged iron line profiles from a  $r=6$  annulus, and for  $30^\circ$ ,  $60^\circ$  and  $85^\circ$  inclination angles (from top to bottom).

the spin of the Black Holes. Pros and cons of these methods are briefly discussed in the following paragraphs.

#### 4.1 Spin

Almost invariably, methods to measure the Black Hole spin make use, directly or indirectly, of the dependence of the ISCO on  $a$ . Methods based on the iron line make no exception. The smaller the inner disc radius, the lower (due to gravitational redshift) the energy to which the profile extends. In Fig. 5, left panel, profiles from accretion discs around a static and a maximally rotating Black Holes, in both cases extending down to the ISCO, are shown. The advantage of this method is that it is very simple and straightforward, at least conceptually. Moreover, no detailed physical modeling of the line emission is required: the spin is measured from the low end of the profile, independently of the exact form of the profile itself (which must be used only to break any degeneracy with the inclination angle).

There are, however, also some limitations and caveats to this method that must be considered. First of all, strictly speaking the method provides only a lower limit to the spin, because the disc (or at least the iron line emitting region) could in principle not extend down to the ISCO. Technically, zero-intensity energies are far from trivial to be measured. Finally, even if the disc (properly said) stops at the ISCO, the region within the ISCO (the so-called plunging region) is not empty, and line emission may arise from the matter free-falling onto the Black Hole (Reynolds & Begelman 1997; Krolik & Hawley 2002), even if matter is expected to be significantly ionized there. If the inner radius

results to be smaller than 2, there is of course no ambiguity. Otherwise, one could always rely to the subtle differences in the profiles due to the metrics themselves (Fig. 5, right panel) which, at least for small radii, are after all not so negligible and will be hopefully exploited by the next generation of large area X-ray satellites.

#### 4.2 Mass (in Active Galactic Nuclei)

Iron  $K\alpha$  reverberation mapping of structures in the profile (Stella 1990) or of integrated quantities (Equivalent Width, centroid energy and width, Matt & Perola 1992) has been suggested, in analogy with the method routinely used for optical broad lines, to measure the BH mass in AGN (this technique is practically unapplicable in Galactic Black Hole systems because of the very short time scales involved, and the much lower typical flux per light-crossing time). It is a conceptually simple but technically very difficult technique. First of all, it requires a lot of photons. Worst than that, the Transfer Function, which describes how the line follows variations of the illuminating continuum, is strongly geometry-dependent. With respect to the BLR reverberation mapping, one here has the advantage that the geometry of the illuminated region can be assumed a priori (i.e. the accretion disc), but has the disadvantage that the geometry of the illuminating region is unknown (in the BLR case a point-like source is a safe assumption, given the much larger distance of the illuminated matter).

On the other hand, if the iron line is emitted in a small spot on the accretion disc (corotating with the disc at the

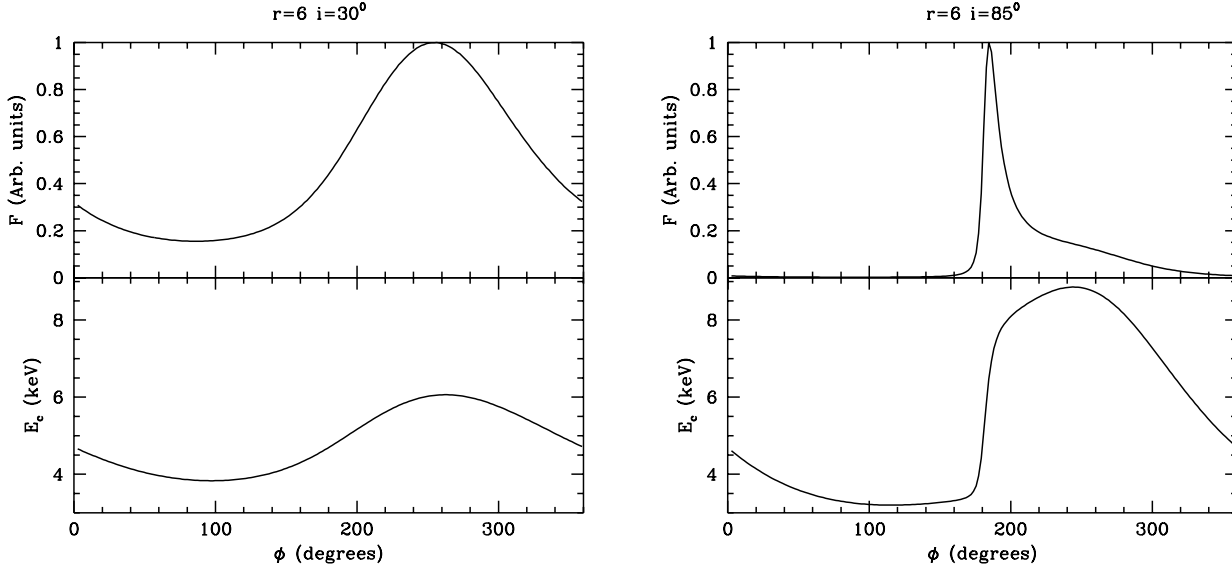


**Fig. 3** Left panel: Flux (upper panel) and centroid energy (lower panel) of the iron line as a function of the azimuthal angle of emission. Radius and inclination angle are 6 and  $30^\circ$ , respectively. Right panel: the same, but for an inclination angle of  $85^\circ$ .

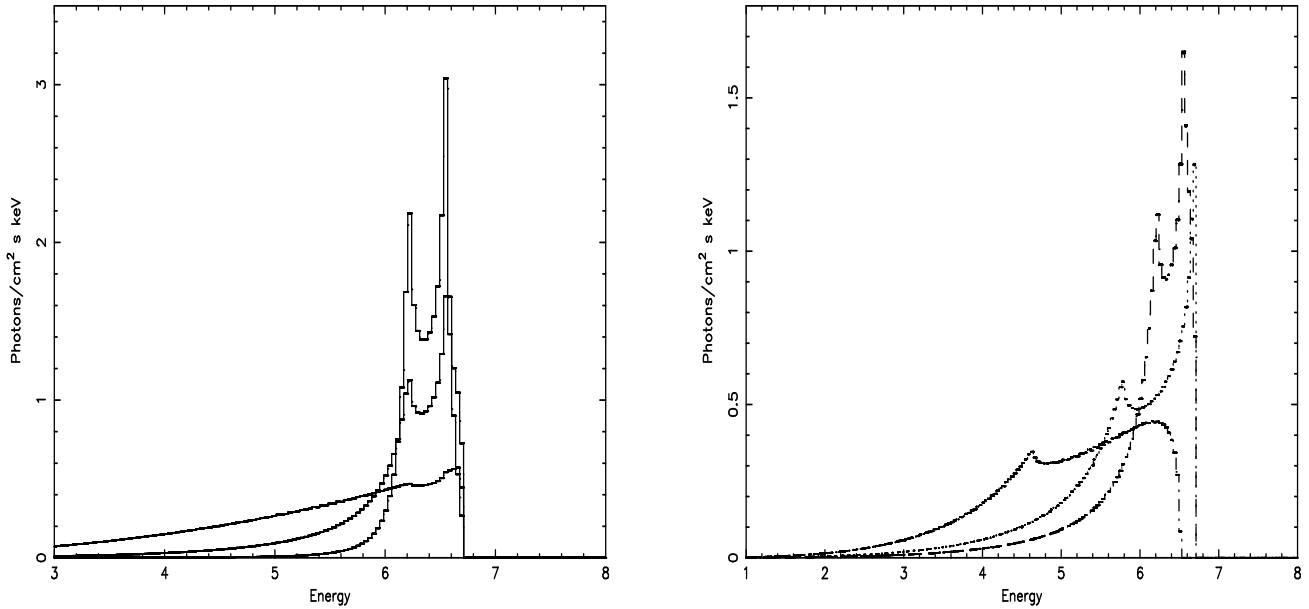


**Fig. 4** Left panel: iron line profiles for a maximally rotating BH, extending from the ISCO to  $400 r_g$ , with a  $30^\circ$  inclination angle. Profiles refer to power law emissivity laws with  $q=1, 2, 3$  (from top to bottom). Right panel: Iron line profiles for a maximally rotating BH, extending from the ISCO to 400, 50 and  $10 r_g$  (from top to bottom) with a  $30^\circ$  inclination angle and  $q=2$ . Here and in the next figure profiles have been calculated with the code KYRLINE (Dovciak et al. 2004a,b) in the XSPEC software package.

Keplerian velocity), the BH mass could be easily and precisely measured, once the spot radius is known (Dovciak et al. 2004c). Such a hot spot may be due to a localized flare, possibly of magnetic origin, just above the disc surface. Because there is some evidence (albeit still controversial) for spot-like emission in AGN (e.g. Turner et al. 2002; Dovciak et al. 2004c; Iwasawa et al. 2004; Pechacek et al. 2005, and references therein), let us discuss this case in some detail.

A spot on the accretion disc at a radius  $r$  has an orbital period (as measured by an observer at infinity) given by:

$$T_{\text{orb}} = 310 \left( r^{\frac{3}{2}} + a \right) M_7 \quad [\text{sec}], \quad (9)$$

where  $M_7$  is the mass of the black hole in units of  $10^7$  solar masses. If the spot radius and the BH spin can be estimated, the measurement of the orbital period immediately provides the Black Hole mass (note that the spin is relevant only for

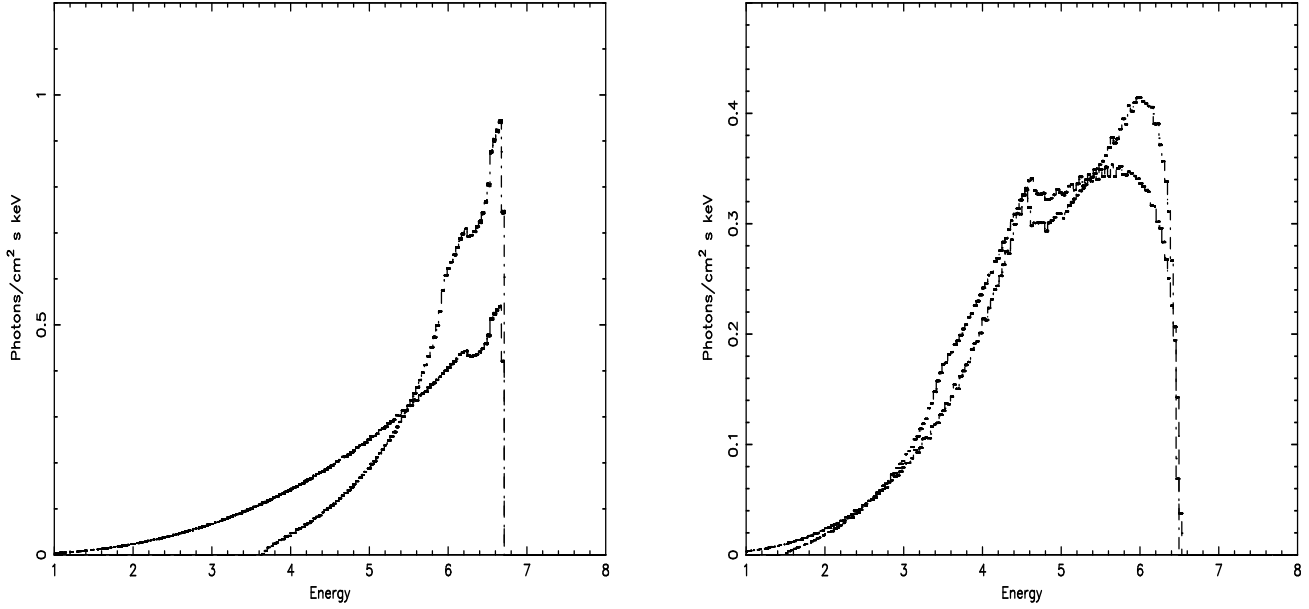


**Fig. 5** *Left panel:* iron line profiles for a maximally rotating BH and a static BH, extending from the ISCO to  $400 r_g$ , with a  $30^\circ$  inclination angle. Note that the profile for the spinning BH extends to much lower energies. *Right panel:* iron line profiles for a maximally rotating BH and a static BH, extending from  $r=2$  to  $10 r_g$ , with a  $30^\circ$  inclination angle, to illustrate the differences due to the metric.

small radii; when  $r \gg 1$ , when the spin is hard to measure, it fortunately becomes irrelevant).

In practice, it is well possible that, in low S/N spectra, only the blue peak is visible (see Fig. 2), resulting in transient and relatively narrow features. For low radii and inclination angles the features may appear redshifted with respect to the rest frame energy. If only the blue peak is visible, and then the entire profile cannot be reconstructed, it will be impossible to tightly constraint the emission parameters, and only allowed intervals for the radius and angle can be derived from the energy shift. To this purpose, Pechacek et al. (2005) found a simple approximated formula which gives, with a very good accuracy, the shift as a function of the radius and the polar and azimuthal angle in the Schwarzschild metric. Calling  $g$  the shift factor, i.e. the ratio between observed (at infinity) and emitted energies, we have:

$$g = \frac{[r(r-3)]^{1/2}}{r + \left[ r - 2 + 4(1 + \cos \phi \sin \theta)^{-1} \right]^{1/2} \sin \phi \sin \theta} \quad (10)$$

where  $\phi$ , as usual, is the azimuthal angle while  $\theta$  is the polar angle (i.e. the inclination angle in case of a disc). In Fig. 6, the maximum and minimum values of the shift factor are shown as a function of the radius for different inclination angles.

## 5 Conclusions

Iron lines are probably the best tools to probe GR effects in the vicinity of Black Holes. Spectral distortions are much easier to study in lines than in continua, because of their intrinsic narrowness - broadening can be safely assume to

arise mainly, when not exclusively, from such effects. Even if many important observational results have already been obtained (as amply discussed in many papers in this volume), much is still to be done, especially in using iron lines to estimate the mass and the spin of the Black Hole. Indeed, relativistic iron lines are still a major scientific driver for next generation, large area X-ray satellites.

*Acknowledgements.* I wish to thank all my collaborators during the more than 15 years in which I've been working in this field. For some of the plots in this paper I have made use of numerical codes developed by M. Dovciak and V. Karas.

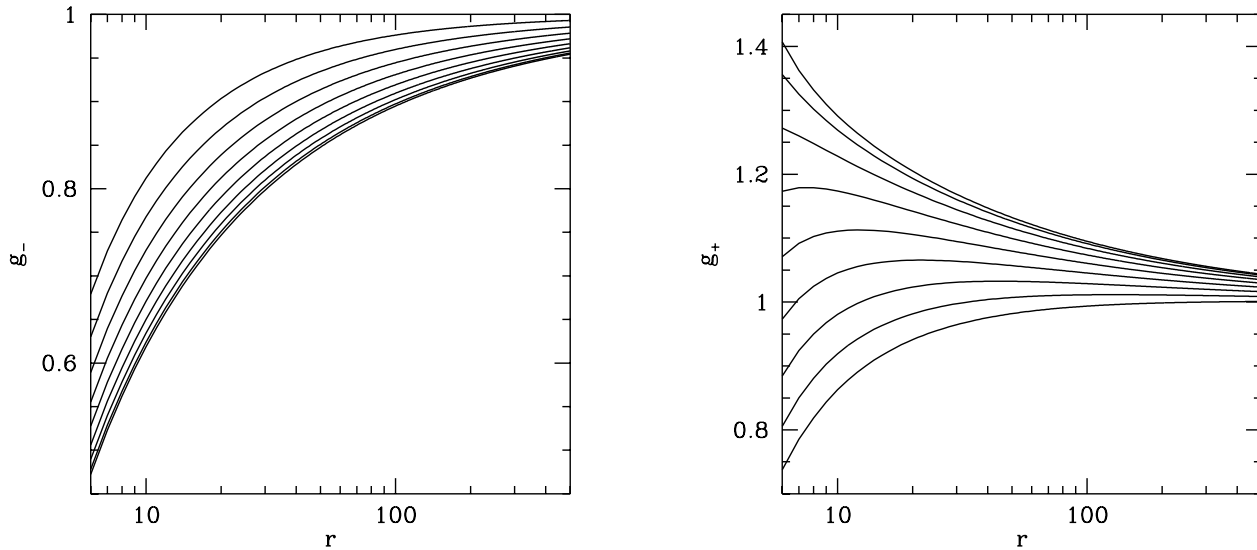


**Fig. 6** The minimum ( $g_-$ , left panel) and maximum ( $g_+$ , right panel) shift factor as a function of radius for 9 different values of the inclination angle:  $5^\circ$ ,  $15^\circ$ , ...,  $85^\circ$  (from top to bottom in the left panel, from bottom to top in the right panel). Calculations, which are for Schwarzschild metric, are based on the analytic, approximated formula (Eq. 10) discussed in Pechacek et al. (2005).

## References

- Arnaud, K.A.: 1996, ASP Conf. Series 101, 17
- Bardeen, J.M., Press, W.H., Teukolsky, S.A.: 1972, ApJ 178, 347
- Beckwith, K., Done, C.: 2004, MNRAS 352, 353
- Beckwith, K., Done, C.: 2005, MNRAS 359, 1217
- Brenneman, L.W., Reynolds, C.S.: 2006, ApJ in press
- Carter, B.: 1968, Phys. Rev. 174, 1559
- Chandrasekhar, S.: 1983, *The Mathematical Theory of Black Holes*, Oxford University Press
- Chen, K., Halpern, J.P., Filippenko, A.V.: 1989, ApJ 339, 742
- Cunningham, C.T.: 1975, ApJ 202, 788
- Di Salvo, T., Iaria, R., Mendez, M., Burderi, L., Lavagetto, G., Robba, N.R., Stella, L., van der Klis, M.: 2005, ApJ 623, L121
- Dovciak, M., Karas, V., Martocchia, A., Matt, G., Yaqoob T.: 2004a, in *Proceedings of RAGtime 4/5 Workshops on black holes and neutron stars*, 14-16/13-15 October 2002/2003, Opava, Czech Republic. Eds: S. Hledk and Z. Stuchlik, Silesian University in Opava, p. 33
- Dovciak, M., Karas, V., Yaqoob, T.: 2004b, ApJSS 153, 205
- Dovciak, M., Bianchi, S., Guainazzi, M., Karas, V., Matt, G.: 2004c, MNRAS 350, 745
- Fabian, A.C., Rees, M.J., Stella, L., White, N.E.: 1989, MNRAS 238, 729
- Fabian, A.C., Iwasawa, K., Reynolds, C.S., Young, A.J.: 2000, PASP 112, 1145
- Fabian, A.C., Miniutti, G.: 2005, in *"Kerr Spacetime: Rotating Black Holes in General Relativity"* eds. D.L. Wiltshire, M. Visser and S.M. Scott, Cambridge Univ. Press
- George, I.M., Fabian, A.C.: 1991, MNRAS 249, 352
- Ghisellini, G., Haardt, F., Matt, G.: 2004, A&A 413, 535
- Iwasawa, K., Miniutti, G., Fabian, A.C.: 2004, MNRAS 355, 1073
- Kerr, R.P.: 1963, Phys. Rev. Lett. 11, 237
- Krolik, J.H., Hawley, J.F.: 2002, ApJ 573, 754
- Laor, A.: 1991, ApJ 376, 90
- Laplace, P.S.: 1796, *Exposition du systeme du monde*, Imprimerie du Cercle Social, an IV, Paris
- Luminet, J.-P.: 1979, A&A 75, 228
- Luminet, J.-P.: 1992, *Black Holes*, Cambridge University Press
- Martocchia, A., Matt, G.: 1996, MNRAS 282, L53
- Martocchia, A., Karas, V., Matt, G.: 2000, MNRAS 312, 817
- Martocchia, A., Matt, G., Karas V.: 2002, A&A 383, L23
- Matt, G., Perola, G.C., Piro L.: 1991, A&A 247, 25
- Matt, G., Perola, G.C.: 1992, MNRAS 259, 433
- Matt, G., Fabian, A.C., Ross, R.R.: 1993a, MNRAS 262, 179
- Matt, G., Perola, G.C., Stella, L.: 1993b, A&A 267, 643
- Matt, G., Fabian, A.C., Ross, R.R.: 1996, MNRAS 278, 1111
- Michell J.: 1783, Phyl. Trans. R. Soc. London 74, 35
- Miniutti, G., Fabian, A.C., Godyer, R., Lazenby A.N.: 2003, MNRAS 344, L22
- Misner, C.W., Thorne, K.S., Wheeler, J.A.: 1973, *Gravitation*, W. H. Freeman editor
- Nandra, K., Pounds, K.A.: 1994, MNRAS 268, 405
- Nayakshin, S., Kallman, T.R.: 2001, ApJ 546, 406
- Palmeri, P., Mendoza, C., Kallman, T.R., Bautista, M.A., Melen-  
dez, M.: 2003, A&A 410, 359
- Pechacek, T., Dovciak, M., Karas, V., Matt, G.: 2005, A&A 441, 855
- Reynolds, C.S., Begelman, M.C.: 1997, ApJ 488, 109
- Reynolds, C.S., Nowak, M.A.: 2003, Phys. Rev. 377, 389
- Ross, R.R., Fabian, A.C.: 2005, MNRAS 358, 211
- Stella, L.: 1990, Nature 344, 747
- Thorne, K.S.: 1974, ApJ 191, 507
- Turner, T.J., Mushotzky, R.F., Yaqoob, T., et al.: 2002, ApJ 574, L123
- Wilms, J., Reynolds, C.S., Begelman, M.C., Reeves, J., Molendi, S., Staubert, R., Kendziorra, E.: 2001, MNRAS 328, L27